

# Periodic volume fluctuations with infinite horizon: Intermittency enhanced Fermi acceleration

Carl P. Dettmann\*

*School of Mathematics, University of Bristol, Bristol BS8 1TW, United Kingdom*

Edson D. Leonel

*Departamento de Física - UNESP - Univ Estadual Paulista, Av.24A,  
1515 - Bela Vista - CEP: 13506-900 - Rio Claro - SP - Brazil*

(Dated: December 24, 2012)

A particle diffuses in a lattice with periodically forced volume. In the finite horizon case with bounded distance between collisions and strongly chaotic dynamics, the velocity growth (Fermi acceleration) is well described by a linear Boltzmann equation, leading to an asymptotic universal non-Maxwellian velocity distribution scaling as  $v \sim t$ . The infinite horizon has intermittent dynamics which enhances the acceleration, leading to  $v \sim t \ln t$  and a non-universal distribution.

Periodically forced thermally isolated systems exhibit many interesting phenomena from stabilization [1] to exponential acceleration [2]. They are of intense interest for trapped atom [3] and ion [4] experiments, as well as astrophysical problems such as transport of comets [5]. Evolving in a spatial coordinate, they also describe transport in periodic structures [6]. Typically there is unbounded growth of the energy, the phenomenon of Fermi acceleration [7] (FA). Very recently, many researchers have sought analytical descriptions of energy distributions in such systems [8–11]. In rather general circumstances a Fokker-Planck (FP) equation can be derived, incorporating the average and variance of the work per period [8]. The first example in [8], extensively investigated elsewhere [9–15] consists of a particle moving freely in a container (“finite billiard”) or amongst obstacles (“Lorentz gas”) with oscillating boundary but fixed volume. Here we relax the fixed volume condition and tame the resulting wild fluctuations in the energy distribution. We consider a variety of regimes distinguished by free paths without collisions (infinite horizon, IH) or lack thereof (finite horizon, FH). Intermittent IH-type motion is found to actually enhance the rate of acceleration, including for the recently introduced “dynamically infinite horizon” [9], that is, IH for only part of each cycle.

Periodically oscillating billiard(-like) models exhibiting Fermi acceleration include the 1D bouncer [16] and stochastic simplified Fermi-Ulam [10] models. In the latter (and often elsewhere), the simplifying assumption of the static wall approximation (SWA) was used, where the boundaries are fixed (hence trivially having fixed volume) but the particle changes its velocity as if it were moving. Many oscillating two-dimensional billiards have also been considered and lead to Fermi acceleration. It is conjectured that this includes all chaotic geometries [14, 15], as well as the ellipse [17]. The breathing case (fixed shape) has been studied in detail [18], leading to slower growth of velocity than other typical models. Fermi acceleration is normally prevented by dissipation in the dynam-

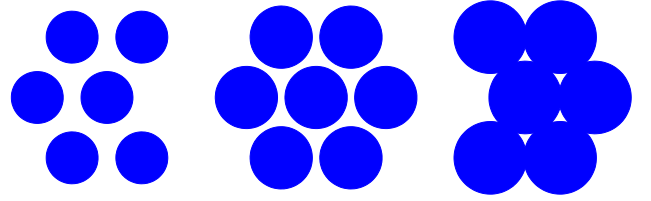


FIG. 1. Part of the triangular Lorentz gas for infinite horizon (IH, left), finite horizon (FH, center), and confined (C, right).

ics, although scaling laws relating the final energy to the strength of the dissipation and other system parameters can be observed [19].

Jarzynski and Swiatecki [12], showed using moments that for fixed volume time-dependent billiards, the eventual distribution of velocities is exponential, in contrast to the Gaussian distribution of an equilibrium gas. Jarzynski [20] then described an FP equation approach for a slowly varying billiard (or fast particle) giving an explicit calculation of the rates of increase of the energy and its variance. Bouchet, Cecconi and Vulpiani [21] in an astrophysical context applied a linear Boltzmann equation to obtain an exponential velocity distribution. More recent innovations have included a hopping wall approximation replacing the SWA [13], and a Chapman-Kolmogorov equation replacing an FP equation [10]. Here we retain the simpler FP approach, but treat the wall collisions exactly. Many of these techniques are also relevant to stochastically moving boundaries, such as the finite temperature Lorentz gas [11, 22].

Our model is a two dimensional Lorentz gas (Fig. 1), which consists of a collection of circular scatterers in an extended domain. Fixed random [23] and periodic [24] scatterer arrangements have been widely studied for the last century. In the periodic case, FH leads to normal diffusion (displacements scale as  $\sqrt{t}$ ), while IH leads to logarithmic superdiffusion ( $\sqrt{t \ln t}$ ). The collision (discrete

time) dynamics is strongly chaotic, with exponential decay of correlations in both FH and IH cases, however the long flights of the IH case leads to  $C/t$  decay of correlations in continuous time.

We place the scatterers on a triangular lattice, with each unit cell having unit area, so the distance between the centres of neighbouring scatterers is  $(4/3)^{1/4}$ . The triangular Lorentz gas is IH for  $r < r_H = (3/64)^{1/4} \approx 0.465$ , FH for  $r_H < r < r_I = (1/12)^{1/4} \approx 0.537$ , at which the scatterers start to intersect, and confined (C) for  $r_I < r < r_B = (4/27)^{1/4} \approx 0.620$  at which point the dynamics is blocked as there is no space outside the scatterers. The area available to the billiard particle is

$$\mathcal{A}(r) = \begin{cases} 1 - \pi r^2 & r \leq r_I \\ 1 - r^2 \left( \pi - 6 \arccos \frac{r_I}{r} + 6 \sqrt{\frac{r^2}{r_I^2} - \frac{r^4}{r_I^4}} \right) & r \geq r_I \end{cases} \quad (1)$$

Here we consider time-dependent scatterers, with radius  $r(t) = R + A \sin t$  and velocity  $u(t) = r'(t) = A \cos t$ ; with suitable scaling this system is equivalent to any other with different lattice spacing and frequency. There are several scenarios depending on  $R_{\pm} = R \pm A$ :

<b>IH:</b> Infinite horizon	$R_+ < r_H$
<b>IFH:</b> Infinite, finite horizon	$R_- < r_H < R_+ < r_I$
<b>IFC:</b> Infinite, finite, confined	$R_- < r_H < r_I < R_+$
<b>FH:</b> Finite horizon	$r_H < R_- < R_+ < r_I$
<b>FC:</b> Finite, confined	$r_H < R_- < r_I < R_+$
<b>C:</b> Confined	$r_I < R_-$

For the numerical simulations we choose  $A = 0.03$ , which allows all the above cases except IFC. A square lattice Lorentz gas has no finite horizon, and so a time-dependent radius would allow IH, C and a further case IC allowing infinite horizon and confined but not finite.

We first discuss Fermi acceleration for the finite or confined geometries. The billiard particle moves freely, colliding with the scatterers according to [18]

$$\mathbf{v}_+ = \mathbf{v}_- + 2\mathbf{n}(u - \mathbf{n} \cdot \mathbf{v}_-) \quad (2)$$

where  $\mathbf{v}_+$  ( $\mathbf{v}_-$ ) is the velocity immediately after (before) the collision,  $\mathbf{n}$  is an outward unit vector normal to the disk at the point of collision, and we use  $v_{\pm} = |\mathbf{v}_{\pm}|$ . The incoming angle  $\theta$  with respect to the normal is defined by  $-\mathbf{n} \cdot \mathbf{v}_- = \cos \theta$ . If the particle with  $v_- < u$  is overtaken by the scatterer then  $\theta > \pi/2$ . We define  $\theta \geq 0$  so there is a 1:1 relation between  $\theta$  and the outgoing speed  $v_+$ ; later this requires an extra factor of two. Eq. (2) gives

$$v_+^2 = \mathbf{v}_+ \cdot \mathbf{v}_+ = v_-^2 + 4uv_- \cos \theta + 4u^2 \quad (3)$$

Thus the change in velocity lies between zero and  $2u$ .

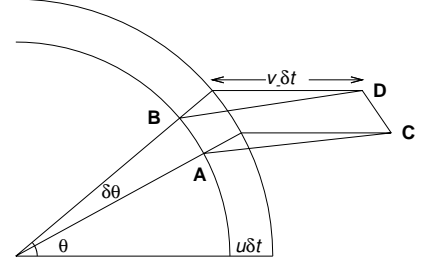


FIG. 2. The particle moves in the negative  $x$  direction. The (almost) parallelogram ABDC denotes the initial positions that will collide in time  $\delta t$ , taking the moving boundary into account.

This system exhibits Fermi acceleration, so almost all initial conditions lead to unbounded velocity; in this regime  $v \gg 1$  and  $v \gg u$ . Thus the particle is effectively in a Lorentz gas with slowly varying radius, and as in the static case, exponential decay of correlations. The only quantity not randomised by the dynamics at short times is  $v$ , which is a constant of motion for the static case.

Thus we may describe the system by a distribution function  $f(v, t)\delta v$  giving the probability of observing the particle with speed in the interval  $[v, v + \delta v]$  at time  $t$ , hence normalised so  $\int_0^\infty f(v, t)dv = 1$  for all  $t$ . The probability of finding the particle in a region of the full phase is, under this assumption,  $f(v, t)\delta v \frac{\delta \psi}{2\pi} \frac{\delta x \delta y}{\mathcal{A}}$  where  $\psi$  denotes the direction of the velocity, including the relevant normalisation factors. Here, and often later, the time dependence of  $r$  (and hence  $\mathcal{A}$ ) has been suppressed.

The distribution  $f(v, t)$  evolves due to collisions with the scatterers, which make small changes of order  $u$  to the speed. The collisions depend on one distribution function and the known position and velocity of the scatterers, so the treatment here is a linear Boltzmann equation, similar to Ref. [21]. This equation ignores correlations between collisions, however we will include their contributions later using the results of Ref. [20].

The general form of a linear Boltzmann equation is

$$f_t = \int [p(v, v')f(v', t) - p(v', v)f(v, t)]dv' \quad (4)$$

where subscript  $t$  (and later  $v$ ) is the partial derivative and  $p(v, v')$  gives the probability density for a collision taking  $v'$  to  $v$ . In our case, we need to compute the probability of a collision taking  $v_- \in [v', v' + \delta v']$  to  $v_+ \in [v, v + \delta v]$  at a time in  $[t, t + \delta t]$  by integrating the distribution over the set of trajectories with the appropriate collision.

For  $r < r_I$  the cross section is independent of  $\psi$ , so we take  $\psi = \pi$ ; larger radii or different chaotic maps would need to take the  $\psi$ -dependence into account. The trajectory hits the scatterer at time  $t$  at a point  $A(r(t) \cos \theta, r(t) \sin \theta)$ ; See Fig. 2. A trajectory

hitting the scatterer at angle  $\theta + \delta\theta$  at time  $t$  reaches it at  $B(r(t)\cos(\theta + \delta\theta), r(t)\sin(\theta + \delta\theta))$ . To reach the scatterer at  $t + \delta t$ , the particle at time  $t$  will be at  $C(r(t+\delta t)\cos\theta + v_-\delta t, r(t+\delta t)\sin\theta)$  or  $D(r(t+\delta t)\cos(\theta + \delta\theta) + v_-\delta t, r(t+\delta t)\sin(\theta + \delta\theta))$  respectively.

We need only leading order in the perturbations, so ABDC is a parallelogram, with area  $r(t)(u + v_- \cos\theta)\delta\theta\delta t$ . We integrate over  $\psi$  but divide by its normalising  $2\pi$ . Thus

$$p(v_+, v_-) = -\frac{2r}{\mathcal{A}}(v_- \cos\theta + u) \left( \frac{\partial\theta}{\partial v_+} \right)_{v_-} \quad (5)$$

where the final derivative comes because we used  $\theta$  to denote the collision variable rather than  $v_+$ ; they are related by Eq. (3). The factor of two comes from considering both positive and negative angles (see above), and the minus sign from the sign of the partial derivative. Substituting for  $\theta$ , we find

$$p(v_+, v_-) = \frac{rv_+(v_+^2 - v_-^2)}{\mathcal{A}u\sqrt{8u^2(v_+^2 + v_-^2) - (v_+^2 - v_-^2)^2 - 16u^4}} \quad (6)$$

Anticipating the expansion in powers of  $u$ , we now write  $v_+ = v_- + 2su$  so that  $s$  ranges in the fixed interval  $[0, 1]$ , and use this in the linear Boltzmann equation

$$\frac{\partial}{\partial t}f(v, t) = \frac{r}{\mathcal{A}} \int_0^1 [p(v, v - 2su)f(v - 2su, t) - p(v + 2su, v)f(v, t)] 2uds \quad (7)$$

For very small velocities ( $v < 2u$ ) we should modify the limits of integration to ensure that the arguments of  $p$  are both positive, however in practice this is not important as we are interested in long times after which the distribution is almost all at large velocities.

We now consider times of order unity, that is, the period of the oscillations. The Boltzmann equation as it stands is not tractable, being explicitly time-dependent. Noting again that for typical particle velocities  $v \gg u$ , we expand the right hand side of the Boltzmann equation in a power series in  $u$ , a Kramers-Moyal expansion [25]. The functions  $f$  and  $p$  are expanded in powers of  $u$ , which then allows the integral to be performed, leading to

$$f_t = \frac{r}{\mathcal{A}} \left[ -\pi u(f + v f_v) + \frac{8u^2 v f_{vv}}{3} + O(u^3) \right] \quad (8)$$

This is now used to determine  $f(v, t)$  at long times. We note that when  $r < r_I$ , ie in the IH, IF and FH cases,  $\dot{\mathcal{A}}/2 = -\pi r u$  is the term that appears in front of the first two terms on the right hand side. Presumably this term is also  $\dot{\mathcal{A}}/2$  for  $r > r_I$ , as in Ref. [20], which gives a comparable equation.[26] Note that terms involving  $u^3$  and higher are significant only for velocities of order  $\sqrt{t}$  or less, thus they do not contribute to the main scaling, which is order  $t$ .

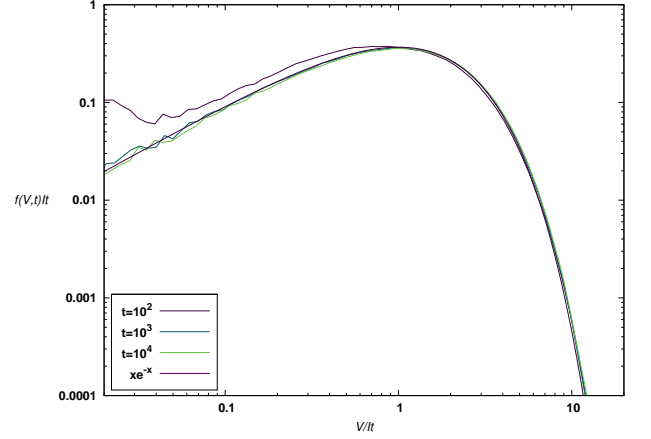


FIG. 3. Convergence to the distribution, Eq. (13) for  $R = 0.5$  (finite horizon).

We now come to the main issue as regards the fluctuating volume. During each oscillation, the particle makes of order  $v$  collisions with the scatterer during each of the expanding and contracting phases, thus increasing and decreasing its speed by amounts of order  $v$ . Based on an approximate averaged equation[27] we propose the following ansatz:

$$f(v, t) = a(t)^2 \frac{v}{t} e^{-a(t)v/t} \quad (9)$$

where  $a(t)$  is bounded and  $2\pi$ -periodic. Substituting into Eq. (8) gives an ODE involving the oscillatory  $r$  and  $u$ :

$$a' = \left( t^{-1} - \frac{\pi u r}{\mathcal{A}} \right) a - \frac{8}{3t} \frac{u^2 r}{\mathcal{A}} a^2 \quad (10)$$

This is a Bernoulli equation, with solution

$$a(t) = t \frac{\sqrt{\mathcal{A}(t)}}{i(t)}, \quad i(t) = \frac{8}{3} \int^t \frac{u^2 r}{\sqrt{\mathcal{A}}} dt' \quad (11)$$

Long time behaviour is characterized by

$$I \equiv \lim_{t \rightarrow \infty} \frac{i(t)}{t} = \frac{4}{3\pi} \int_0^{2\pi} \frac{u^2 r}{\sqrt{\mathcal{A}}} dt, \quad (12)$$

an elliptic integral depending on  $R$  and  $\mathcal{A}$  that is easy to evaluate numerically [28]. Thus our final expression for the velocity distribution function is

$$F(V, t) = \frac{V}{I^2 t^2} e^{-V/(It)} \quad (13)$$

where  $V = v\sqrt{\mathcal{A}}$  and  $F(V, t)dV = f(v, t)dv$ . More generally, in an adiabatic compression we expect the entropy to be roughly invariant, and indeed it is just a function of  $V$  for this two dimensional ideal gas. Thus in thermally isolated systems with fluctuating volume the entropy, rather than energy or velocity, is the primary variable.

This distribution is confirmed numerically in Fig. 3 for  $R = 0.5$  and  $\mathcal{A} = 0.03$ , so the FH regime. For this case

numerical integration gives  $I = 0.001327658$ . We simulate the full (not SWA) time-periodic Lorentz gas. Determining the time until the next collision thus involves the solution of a transcendental equation, using the robust quadratically convergent method proposed in [16]. A million initial conditions of particles are chosen using a Maxwell-Boltzmann distribution at a temperature of  $10^{-4}$  consistent with  $|u| < A = 0.03$ . Particles which are very slow may not collide during the simulation time, and so delay convergence to the limiting distribution. Note that  $A$  more than doubles over the cycle and would be clearly visible in Fig. 3 if not incorporated correctly.

Next, we consider infinite horizon. Here, the correlations are non-integrable, so the Boltzmann equation cannot be applied, and in general the velocity distribution is non-universal. We will however determine the scaling of velocity with time. There are two cases, IH (pure infinite horizon) and IF (infinite-finite, also called dynamically infinite). In the IF case the time of free flights is bounded by the period, but since the velocity can be arbitrarily large, the distance is not bounded. In spite of the long flights, most particles at any given time have collided much more recently than an oscillation period, so the velocity distribution is still approximately a function of  $V$  as before (see Eqs. 1, 13).

For both IH and IF we expect the Fermi acceleration to be of the form  $v \sim t \ln t$ , as follows: Consider a flight of time  $\tau$  between successive collisions. The probability a flight of length between  $\tau$  and  $\tau + d\tau$  is (neglecting multiplicative constants) of order  $(v\tau)^{-3}d(v\tau) = v^{-2}\tau^{-3}d\tau$  for  $\tau \gg v^{-1}$ , the typical flight time. See eg Ref. [24] for computation of the constant in the static case.

Collisions normally occur with a rate  $\approx v$ , so a long flight avoids a change of velocity  $\approx v\tau$  to the particle, noting that  $u$  is at most of order unity. Thus the perturbation  $\delta \ln v = \delta v/v$  is of order  $\tau$ . The effects are however effectively uncorrelated, so we must add variances, which appear in proportion to their probability

$$\sum (\delta \ln v)^2 \approx \int_{v^{-1}}^1 v^{-2} \tau^{-3} \tau^2 d\tau \quad (14)$$

The lower limit of integration is the typical time  $v^{-1}$  and the upper can be taken as the largest time found in the trajectory, however there is no extra velocity perturbation for free paths of time greater than the period (of order 1). Thus we find that per collision the variance scales as  $\ln v/v^2$ . The number of collisions required to reach paths of order unity is about  $v^2/\ln v$ , which is less than the simulation time, noting that in the finite horizon case the Fermi acceleration is of order  $v \sim t$ .

The particle thus undergoes a random walk in  $\ln v$ , taking a number of collisions  $v^2/\ln v$ , and hence a time  $v/\ln v$  to take each step. The total time for the trajectory is dominated by the largest value of  $v$  in the path, so that the velocity is typically of order  $t \ln t$ . This argument follows through for both infinite (I) and infinite/finite (IF)

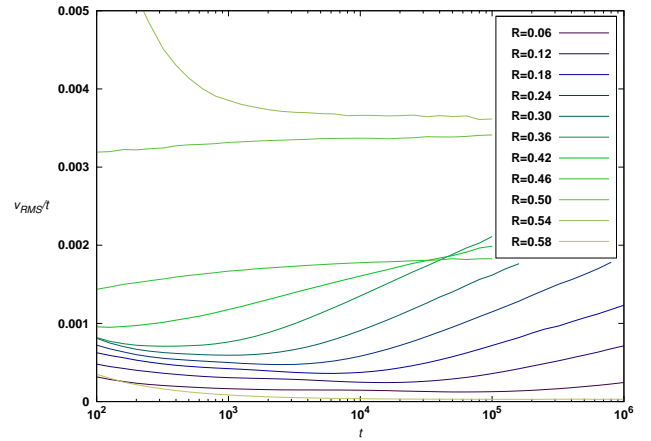


FIG. 4. Velocity growth for different  $R$ . The curves start horizontal ( $v \sim t$ ), and those with  $R < 0.45$ , where the infinite horizon is noticeable, then increase linearly ( $v \sim t \ln t$ ). The lowest curve,  $R = 0.58$ , is a billiard completely confined for all time, exhibiting the weakest Fermi acceleration.

cases, although it is more pronounced (larger coefficient) in the former. Note also the paradoxical effect in which the intermittency leading to a long time without collisions is actually responsible for increasing the (collision-driven) Fermi acceleration.

The dependence of the Fermi acceleration on the radius (and hence the finite/infinite horizon status) is shown in Fig. 4. Here the quantity plotted is the root mean square velocity. In time, the regimes are (a) dominated by the initial Maxwell-Boltzmann distribution, (b) linear growth of  $v$ , (c) for IH, increase as the logarithmic Eq. (14) starts to dominate the normal linear acceleration. The transitions depend on the coefficients of the relevant terms, moving to shorter times as the radius is decreased.

The FC parameter range, in which the particle is alternately confined and unconfined, needs further study. In particular, it is interesting to investigate the many rapid collisions undertaken by a particle near where the two scatterers touch, a new “dynamical cusp” mode of intermittency. The possibility of an unbounded number of collisions suggests that since in each (approximately perpendicular) collision, a fixed quantity  $u$  is added to the velocity, the velocity itself can become unbounded in finite time for a small set of initial conditions, a further example of intermittency enhanced acceleration.

The authors are grateful for support from Brazilian agencies FAPESP, FUNDUNESP and CNPq. This research was supported by resources supplied by the Center for Scientific Computing (NCC/GridUNESP) of the São Paulo State University (UNESP).

\* <http://www.maths.bris.ac.uk/~macpd>

- [1] I. Gilary, N. Moiseyev, S. Rahav, and S. Fishman, Journal of Physics A: Mathematical and General **36**, L409 (2003).
- [2] V. Gelfreich, V. Rom-Kedar, K. Shah, and D. Turaev, Phys. Rev. Lett. **106**, 074101 (2011).
- [3] T. Salger, S. Kling, T. Hecking, C. Geckeler, L. Morales-Molina, and M. Weitz, Science **326**, 1241 (2009).
- [4] C. Ospelkaus, C. E. Langer, J. M. Amini, K. R. Brown, D. Leibfried, and D. J. Wineland, Phys. Rev. Lett. **101**, 090502 (2008).
- [5] I. I. Shevchenko, New Astronomy **16**, 94 (2011).
- [6] E. D. Leonel, D. R. da Costa, and C. P. Dettmann, Physics Letters A **376**, 421 (2012).
- [7] E. Fermi, Phys. Rev. **75**, 1169 (1949).
- [8] G. Bunin, L. D'Alessio, Y. Kafri, and A. Polkovnikov, Nature Physics **7**, 913 (2011).
- [9] A. K. Karlis, F. K. Diakonov, C. Petri, and P. Schmelcher, Phys. Rev. Lett. **109**, 110601 (2012).
- [10] A. K. Karlis, F. K. Diakonov, and V. Constantoudis, Chaos **22** (2012).
- [11] L. D'Alessio and P. L. Krapivsky, Physical Review E **83**, 011107 (2011).
- [12] C. Jarzynski and W. Swiatecki, Nuclear Physics A **552**, 1 (1993).
- [13] A. K. Karlis, P. K. Papachristou, F. K. Diakonov, V. Constantoudis, and P. Schmelcher, Phys. Rev. E **76**, 016214 (2007).
- [14] A. Loskutov, A. Ryabov, and L. Akinshin, Journal of Experimental and Theoretical Physics **89**, 966 (1999).
- [15] A. Loskutov, A. B. Ryabov, and L. G. Akinshin, Journal of Physics A: Mathematical and General **33**, 7973 (2000).
- [16] C. P. Dettmann and E. D. Leonel, Physica D-Nonlinear Phenomena **241**, 403 (2012).
- [17] F. Lenz, F. K. Diakonov, and P. Schmelcher, Phys. Rev. Lett. **100**, 014103 (2008).
- [18] B. Batisti and M. Robnik, Journal of Physics A: Mathematical and Theoretical **44**, 365101 (2011).
- [19] D. F. M. Oliveira, J. Vollmer, and E. D. Leonel, Physica D-Nonlinear Phenomena **240**, 389 (2011).
- [20] C. Jarzynski, Phys. Rev. E **48**, 4340 (1993).
- [21] F. Bouchet, F. Cecconi, and A. Vulpiani, Phys. Rev. Lett. **92**, 040601 (2004).
- [22] G. Gradenigo, A. Puglisi, A. Sarracino, and U. M. B. Marconi, Phys. Rev. E **85**, 031112 (2012).
- [23] H. V. Kruis, D. Panja, and H. van Beijeren, Journal of Statistical Physics **124**, 823 (2006).
- [24] C. P. Dettmann, Journal of Statistical Physics **146**, 181 (2012).
- [25] H. Risken and H. D. Vollmer, Zeitschrift für Physik B Condensed Matter **66**, 257 (1987), 10.1007/BF01311663.
- [26] The  $f_{vv}$  term in Eq. (8) is of the same form as the diffusive term in Ref. [20] (substituting energy  $E = mv^2/2$  and mass  $m = 1$ ), but has a different coefficient, for two reasons: Ref. [20] neglects the effect of motion of the boundary on the collision rate ("aberration," Fig. 2). In addition we assume independence of collisions, good for the Lorentz gas except very close to  $r_I$ . In detail, Eqs. (3.12, 3.16a, 3.22a) of Ref. [20] give the same as in Eq. (8) but with  $8u^2/3$  replaced by  $4 \sum_{j=-\infty}^{\infty} c_j$  where  $c_j$  is the autocorrelation of the function  $u \cos \theta - \langle u \cos \theta \rangle$  in our notation, and here  $u$  is independent of position. The main term is  $4c_0 = (8/3 - \pi^2/4)u^2$ , given (correctly) in Eq. (A7). The other correlations are small, for example, the largest term for  $r = 0.53$ , just less than  $r_I$ , is  $4c_3 \approx 0.008$ . The numerical simulations in Fig. 3 are consistent with  $8/3$  plus undetectable correlation corrections, but not with  $8/3 - \pi^2/4$ . If desired, we can incorporate the other  $c_j$  into our approach directly. The Boltzmann equation fails for infinite horizon, however, since in this case  $\sum c_j = \infty$ .
- [27] If we average Eq. (8) by neglecting the  $u$  terms (which are full time derivatives) we find  $\bar{f}_t = 8Cv\bar{f}_{vv}/3$  where  $C$  is the average of  $u^2/\mathcal{A}$ , leading to  $\bar{f}(v, t) = 9ve^{-3v/(8Ct)}/(64C^2t^2)$ . However this cannot capture the fluctuations in  $f$  that take place each period.
- [28] J. A. C. Weideman, American Mathematical Monthly **109**, 21 (2002).